Effect of electronic alignment upon the reaction $2Na^*(^2P_{3/2}) \rightarrow Na_2^+ + e^-$

Erhard W. Rothe and R. Theyunni
Research Institute for Engineering Sciences and Department of Chemical Engineering, Wayne State University, Detroit, Michigan 48202

Gene P. Reck and C. C. Tung
Department of Chemistry, Wayne State University, Detroit, Michigan 48202

(Received 22 October 1984)

The $3p$ electrons of Na^* are aligned with the use of a single-mode linearly polarized laser. The reaction occurs at subthermal kinetic energy in a single atomic beam. The ion yield decreases by $\sim 50\%$ when the electric vector of the light is rotated 45° from a direction parallel to the sodium beam. A polarization effect for this reaction has been previously described and our data disagree with those results.

INTRODUCTION

The associative ionization of two excited sodium atoms,

$$2Na^*(3^2P_{3/2}) \rightarrow Na_2^+(X^2\Sigma_g^+) + e^- , \quad (1)$$

has been previously observed in vapor[1] and in beams.[2] The reaction has just sufficient energy to reach $v=3$ of the ion.[3] We describe here a measurement of the dependence of the ionization cross section upon the alignment of the two Na^*. The experiment is similar to that described by Kircz, Morgenstern, and Nienhuis (KMN),[4] but the results do not agree.

EXPERIMENT

A schematic of the apparatus is in Fig. 1. The terms ray and beam describe directed photons and atoms, respectively. A single sodium beam is generated from a cw nozzle source which is identical to that of Ref. 5. The Na^* collide because there is a distribution of speeds within that beam. This implies that (a) the relative kinetic energies are subthermal and (b) the relative velocities v_r are parallel to the beam. The sodium source is in a chamber whose pressure is $\sim 1\times 10^{-6}$ Torr. The ray and beam intersect in a second chamber, and a surface-ionization Na-beam monitor is located in a third. These chambers have pressures of $\sim 1\times 10^{-7}$ Torr.

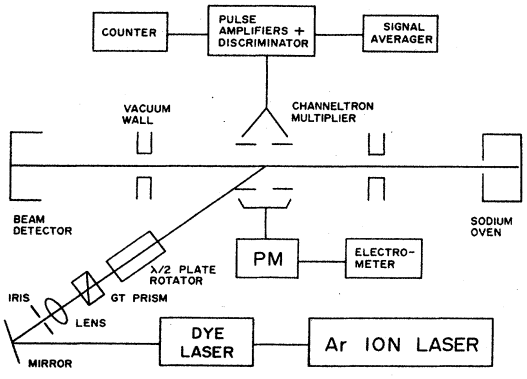

FIG. 1. Schematic of the experiment. Drawing is not to scale. Variations upon this arrangement are described in the text.

The Na^* are created with linearly polarized single-mode light from a stabilized dye laser (Coherent model 599-21), via the standard[5-7] excitation scheme involving the $3^2S_{1/2}(F=2) \leftrightarrow 3^2P_{3/2}(F=3)$ transition near 589 nm. There are many excitations for each atom, which yields an aligned stationary-state distribution of the magnetic quantum number m_F. The populations are 0, $\frac{1}{42}$, $\frac{10}{42}$, $\frac{20}{42}$, $\frac{10}{42}$, $\frac{1}{42}$, and 0, for $m_F=-3$, -2, -1, 0, 1, 2, and 3, respectively. The quantization axis is the electric vector **E** of the light. The conditions required to reach this stationary state have been extensively discussed by Fischer and Hertel[7] and are achieved here.

The ray and the beam are perpendicular, and their directions define coordinates **X** and **Z**, respectively. Some fluorescence from the Na^* strikes one end of a 3-mm-diam optical-fiber bundle, which is located about 10 mm in the $-\mathbf{Y}$ direction from the **X**-**Z** intersection. The fluorescence is used to adjust and to monitor the laser frequency. A typical full width at half maximum of the intensity is 25 MHz.

In a separate experiment we mass analyzed the ions and they were all Na_2^+, in agreement with the energetics[3] and with previous results.[2] There is a $\sim \frac{1}{2}$ G magnetic field in the intersection region. Fisher and Hertel[7] have shown that this has little effect upon the Na^* alignment. There is also a static electric field in this region of ~ 100 V/cm, which accelerates the ions toward a channeltron located ~ 15 mm in the $+\mathbf{Y}$ direction from the **X**-**Z** intersection. This field also increases the exoergicity slightly. The channeltron's output is processed by an emitter follower, an amplifier, and a discriminator. The resulting standard pulses go to a signal averager (Fabri-Tek, Model 1062) operating in a multiscalar mode and to a counter. The Na_2^+ count rate $\dot{I}$ is also sometimes used to tune the laser: There is excellent agreement between the two methods.

The experiment yields the number of Na_2^+ produced, I, as a function of the direction of **E**, which makes an angle θ in the **Y-Z** plane with **Z**. We rotate θ, at 72°/s, by turning a $\lambda/2$ plate with a synchronous motor. A 360° rotation of the plate corresponds to a 720° change in θ. A trigger signal from the rotator, at θ_0, starts a sweep of 256 channels in the signal averager. We usually use a dwell time of 50 ms/channel so that a sweep corresponds to 922° in θ. The next sweep is triggered at $\theta_0+1440°$.

The $\dot{I}$ are in the range of 100—2000 Hz (the dark count rate is typically 10 Hz), and $I(\theta)$ is accumulated in 10—100 sweeps. If the laser frequency drifts, i.e., when $\dot{I}$ decreases ~30%, we interrupt the sweeps and retune the laser. The accumulated $I(\theta)$ are transferred to a computer.

We use 10—50 mW of single-mode laser power. The ray diameter is usually ~10 mm through the Na beam. In some experiments a focusing lens reduces its diameter to ~2 mm. Although this changes $\dot{I}$, it does not affect the shape of $I(\theta)$. Alternatively, an iris is used to remove the Gaussian wings of the ray so that non-stationary-state distributions of Na* at these edges could be avoided.[7] This also failed to change $I(\theta)$.

The ray is sent through a Glan prism so that it is completely linearly polarized. Subsequently it goes through the $\lambda/2$ plate and enters the vacuum chamber via a glass window at normal incidence. Ocassionally a Glan prism is placed after the $\lambda/2$ plate. This serves two purposes. When **E** is rotating, the ray intensity at the intersection region is totally attenuated when $\theta=0°$ and so (a) the position corresponding to minimum I yields an absolute value for θ and (b) I is a measure of the dark counts.

Care is taken to adjust the $\lambda/2$ plate to be perpendicular to the ray. It is adjusted so that the reflections from the rotating plate move in a circle about the ray. If this is improperly done, the ray-beam intersection volume moves and results in different I for equivalent directions of **E**. For example, at θ and $\theta+360°$ (i.e., a 180° turn of the $\lambda/2$ plate), $I(\theta)/I(\theta+360°)$ has been as large as two. That is why we usually obtain data for a large range of θ (i.e., 922°), rather than the 90° which would otherwise be adequate. We initially used a double Fresnel rhomb (Spectra Physics Model 310) in place of the $\lambda/2$ plate. Although the rhomb produces greater spatial variations, the $I(\theta)$ was the same.

Fischer and Hertel[7] recommend that the fluorescence intensity be measured as a function of θ in order to establish that there is a stationary-state distribution of m_F. We sometimes measure ratios of fluorescence intensities at $\theta=0°$ and 90°. While these are consistent with stationary-state conditions, we do not know the polarization dependence of the optical-fiber input, and so we rely instead upon (a) the fact that our $I(\theta)$ are independent of laser power and power density and (b) the fact that our spectral densities, with the 25-MHz laser half-width, are well within saturation conditions calculated and measured by others.[6,7]

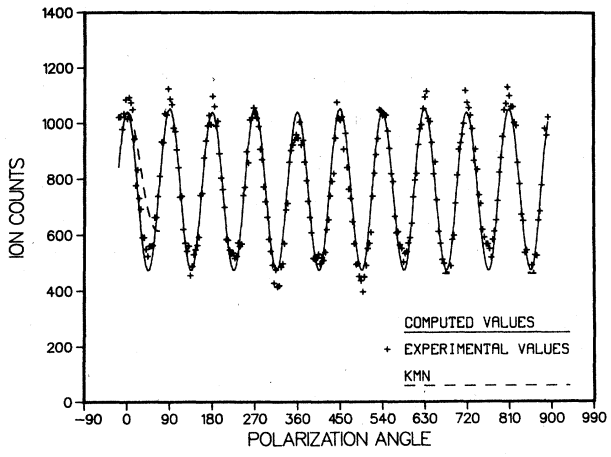

FIG. 2. A typical data set for $I(\theta)$. The + represents the raw-data points (the number of Na_2^+ ions), the solid line is our normalized fit to those points, while the dashed line is the fit of KMN to their data. Both fits are to the form $R_0+R_1\cos(2\theta)+R_2\cos(4\theta)$.

RESULTS

Typical raw data are displayed in Fig. 2. This shows $I(\theta)$ to have maxima every 90° and essentially $I(\theta)\propto\cos(4\theta)+$ const. In contrast, a qualitative look at the KMN (Ref. 4) data suggests their maxima are separated by 180°, so that $I(\theta)\propto\cos(2\theta)+$ const.

More quantitatively, KMN fitted their normalized data to

$$I(\theta)=1+r_1\cos(2\theta)+r_2\cos(4\theta)\,, \tag{2}$$

with $r_1=0.27$ and $r_2=0.10$. In contrast, from the data in Fig. 2, we obtain $r_1=-0.01\pm0.01$ and $r_2=0.38\pm0.01$. This means that (a) we obtain a larger polarization effect—KMN reported 1.7 for I_{max}/I_{min} while we measure 2.2—and (b) we obtain essentially half their "wavelength" in $I(\theta)$. The fits to our $I(\theta)$, and the KMN fit to theirs, are shown in Figs. 2 and 3.

We have no satisfactory explanation for this discrepancy. However, we discuss below three conceivable causes of error.

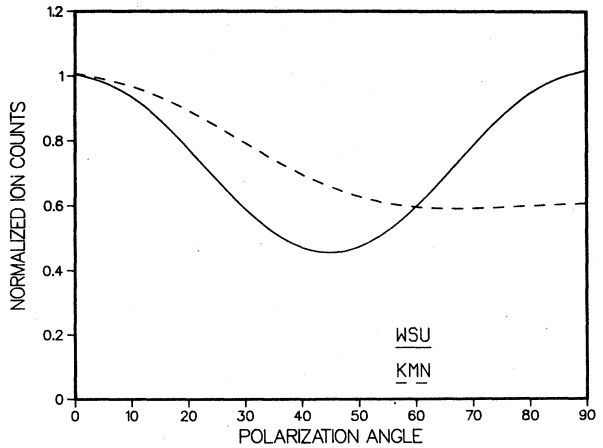

FIG. 3. Expanded plot of the fits to our $I(\theta)$ and the KMN fits to theirs, normalized to unity at $\theta=0$.

(a) Attainment of stationary state. KMN measured the dependence of fluorescence intensity upon θ and reported that they had a stationary state. As explained previously, we did not rely upon this method. However, because the stationary-state distribution has the largest degree of alignment attainable from linearly polarized light,[7] a failure on our part to attain the stationary state would have produced a smaller polarization effect than KMN and not the larger one observed.

(b) Radiation trapping. Fisher and Hertel[7] have emphasized that excessive Na density leads to radiation trapping and thus to reduced alignment. We can estimate our density within an order of magnitude, based on the beam geometry, the Na speeds, and the measured beam intensity. It is less than 10^9 atoms/cm^3, well below the optical trapping regime.[7] Furthermore, we obtain approximately the same $I(\theta)$ with experiments conducted with an order-of-magnitude range of beam densities. In any case, optical trapping would reduce the polarization effect, not increase it.

(c) Error in ion measurement. One possible source of error would be fluorescence photons that are mistaken for ions at the channeltron, i.e., that eject electrons at its input. This could happen if the surfaces become partially covered with Na, thereby reducing the work function. Because the fluorescence intensity at the channeltron has maxima and minima at $\theta=0°$ and 90°, respectively, this would enhance the spurious I counts at 0°. *If* this error has occurred in the KMN experiment, it could explain the discrepancy. However, Morgenstern and Nienhuis state (private communication) that they proved that this did not occur.

DISCUSSION

Estimates for relevant potential-energy (PE) curves are shown in Fig. 4. There is no direct information about the twelve possible PE curves between two $3p$ sodium atoms, and so we adapt those calculated by Konowalow and Fish[8] for the $2p$-$2p$ interactions in Li_2. For Na_2, the PE of the $3p$-$3p$ asymptote[3] is 0.05 eV greater than that of $v=0$, $J=0$ of Na_2^+. In contrast, the PE of Li_2^+ lies above the $2p$-$2p$ asymptote and so the lithium analog of reaction 1 is endoergic. Our adaptation in Fig. 4 consists of (a) lowering the Li_2^+ well so as to be 0.05 eV below the $2p$-$2p$ asymptote and (b) deleting ten "nonrelevant" Na_2 curves, as described below.

Consider Fig. 4. The Na_2^+ is presumably formed via a PE crossing of Na_2^+ and Na_2. Only the $^2\Sigma^+$ ground state of Na_2^+ is energetically accessible. There are narrow energy limits which reduce the choice for Na_2 from twelve PE curves to two. On one hand, the collision energies are $\lesssim 0.02$ eV, so that crossings which lie at PE greater than that, relative to the asymptote, cannot contribute. On the other hand, the maximum exoergicity is ~ 0.05 eV, which excludes attractive curves which lie below the ionic potential.

Figure 4 contains the $^1\Sigma_g^+$ and $^3\Delta_u$ PE curves for Na_2 because only these *might* meet the two criteria listed above. Because of the uncertainty in the adaptation from the Li_2, we do not know whether they do: As pictured in

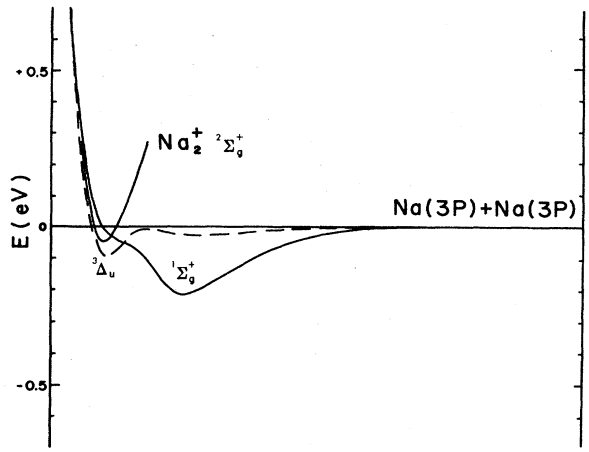

FIG. 4. The two relevant Na_2 PE curves and that for Na_2^+. These curves are estimated (see text) and so it is not known whether there are zero, one, or two neutral-ionic crossings.

Fig. 4, only one of them crosses the Na_2^+ curve. However, based on the similarity between other analogous PE curves for Li_2 and Na_2, it seems very unlikely that any of the other ten PE curves contribute. (Konowalow and Fish[8] suggest that a $^3\Sigma$ state is responsible for the analogous reaction with lithium, where the ionic well lies above the $2p$-$2p$ asymptote so that more kinetic energy would be required.)

Consider two Na* whose internuclear separation R is very large. This implies that the relative alignment of the lobes is fixed only by **E** because (a) the impact parameter is negligible compared to R and (b) the interaction between the lobes is too small to disturb their mutual positions. Of the two potentials described above, the $^1\Sigma_g^+$ is the result of the interaction of two atoms with $m_l=0$, the $^3\Delta_u$ with both m_l either $+1$ or -1.

When $\theta=0$, i.e., when **E** is parallel to the beam, then the p lobes produced in the excitation lie primarily along laboratory coordinate Z, which is parallel to v_r, so that $m_l=0$, and so the Na* would approach each other along v_r with the p lobes also pointing along v_r. This is the textbook picture of the alignment of two p_z orbitals which form σ bonds and is responsible for the $^1\Sigma_g^+$ asymptote. In the same vein, when $\theta=90°$, the $^3\Delta$ state is formed when both m_l are either $+1$ or -1, and we may expect π orbitals.

The excitation process with linearly polarized light does not actually produce the pure m_l states implied above. The stationary-state distribution of m_F can also be converted to that of m_j or m_l. It has been shown[9] that the distribution of m_l with respect to the original quantization axis **E** can be transformed into another with respect to **R**. For one Na* the probability $w(m_l)$ of obtaining $m_l=0$ or ± 1, with respect to **R** (at large R), is $w_\infty=(\frac{2}{3}+\cos^2\theta)/3$ and $w_8=(\frac{7}{3}-\cos^2\theta)/3$, respectively.[9] The asymptotic behavior of two Na* is obtained from joint probabilities. These are $w_{\infty\infty}$ $(=w_\infty^2)$, w_{88} $(=w_8^2)$, and $w_{\infty 8}=2w_8w_\infty$; e.g., $w_{\infty\infty}$ is the probability both Na* have $m_l=0$ along **R** at large R.

All 12 neutral PE curves correspond asymptotically to

one of these three alignments. We tried to match an equation of the form $I(\theta)=cw_{\infty\infty}+dw_{88}+ew_{\infty 8}$, where c, d, and e are probabilities to form Na_2^+ from the respective alignments, to that used in Eq. (2). These two forms of $I(\theta)$ are equivalent and the ratios of c/d ($\equiv c^*$) and e/d ($\equiv e^*$) can be calculated from r_1 and r_2. Unfortunately for this approach, our fit yields $c^*=2.26$ and $e^*=-1.23$ while that of KMN produces $c^*=3.37$ and $e^*=-0.46$, respectively. The negative probabilities imply that the model is wrong. Similarly, if we follow our previous suggestion that only the two PE for Na_2 displayed in Fig. 4 can contribute, then $e^*=0$, and the algebra shows that c^* can be derived from either r_1 or r_2. Our fit yields the inconsistent results that $c^*=1.52$ and -2.73 from r_1 and r_2, respectively, while the analogous KMN results are 3.62 and -9.47. KMN analyzed their data via an m_j approach (rather than the m_l used here). They obtained positive rate coefficients: However, use of their treatment with our r_1 and r_2 yields negative values (see note added in proof).

The actual situation is more complicated than our simple model. For example, at a finite impact parameter, two p lobes which initially are in a σ alignment at large R will be in a π alignment at the minimum R,[10] if there is no interaction between them. In addition, at some value of R the orbitals will begin to interact and then they will start to align themselves with respect to **R** rather than **E**. We have not analyzed this further.

CONCLUSIONS

Our data for this reaction are very different from those reported by KMN. The experimental arrangements are, in principle, almost identical. We have varied Na densities, laser intensities and geometries over wide ranges, and have investigated all reasonable parameters. We still have no good explanation for the experimental discrepancy. A model based on the asymptotic behavior of the m_l fails to explain either set of data and further work is needed to explain (a) the magnitude of the effect and (b) its angle dependence.

Note added in proof. The recent analysis by H. P. Saha, J. S. Dahler, and D. M. Jones, Phys. Rev. A **30**, 1345 (1984) of the KMN data fails to fit ours.

ACKNOWLEDGMENTS

The research was supported by the National Science Foundation under Grant No. CPE-81-06325. Mr. Seong-Poong Lee helped with the data processing. We also acknowledge helpful conversations with R. Düren, H. Tischer, L. Hüwel, D. Konowalow, H. Pauly, and J. Weiner.

[1]A. Klyucharev, V. Sepman, and V. Vuinovich, Opt. Spektrosk. **42**, 588 (1977) [Opt. Spectrosc. **42**, 336 (1977)]; F. Roussel, B. Carré, P. Breger, and G. Spiess, J. Phys. B **14**, L313 (1981); V. S. Kushawaha and J. J. Leventhal, Phys. Rev. A **22**, 2468 (1980); **25**, 346 (1982); J. Huennekens and A. Gallagher, Phys. Rev. A **28**, 1276 (1983).

[2]A. A. de Jong and F. v. d. Valk, J. Phys. B **12** L561 (1979); J. Weiner and P. Polack-Dingels, J. Chem. Phys. **74**, 508 (1981); R. Bonanno, J. Boulmer, and J. Weiner, Phys. Rev. A **28**, 604 (1983).

[3]The $v=3$ and $v=4$ levels of ground electronic state Na_2^+ have 39836 ± 2 and 39954 ± 2 cm^{-1} more energy, respectively, than does $v=0$, $J=0$ of the Na_2 X state, S. Leutwyler, T. Heinis, H. P. Härri, and E. Schumacher, J. Chem. Phys. **76**, 4290 (1982). $D_0^0(Na_2)=(6024-78)\pm6$ cm^{-1}, K. K. Verma, J. T. Bahns, A. R. Rajaei-Rizi, W. C. Stwalley, and W. T. Zemke, J. Chem. Phys. **78**, 3599 (1983). $Na^*(3^2P_{3/2})$ has 16973.4 cm^{-1} more energy than Na, P. Risberg, Ark. Fys. **10**, 591 (1956). Thus the exoergicity for reaction 1, to $v=3$ of ground state Na_2^+, is $[2\times16973.4+(6024-78)-39836]$ cm^{-1} $=56.8\ (\pm7)$ cm^{-1}.

[4]J. G. Kircz, R. Morgenstern, and G. Nienhuis, Phys. Rev. Lett. **48**, 610 (1982); see also G. Nienhuis, Phys. Rev. A **26**, 3137 (1982).

[5]R. Düren and H. O. Hoppe, J. Phys. B **11**, 2143 (1978).

[6]I. V. Hertel and W. Stoll, Adv. At. Mol. Phys. **13**, 113 (1978).

[7]A. Fischer and I. V. Hertel, Z. Phys. A **304**, 103 (1982).

[8]D. D. Konowalow and J. L. Fish, Chem. Phys. **84**, 463 (1984); **77**, 435 (1983).

[9]L. Hüwel, J. Maier, and H. Pauly, J. Chem. Phys. **76**, 4961 (1982).

[10]W. Reiland, G. Jamieson, U. Tittes, and I. V. Hertel, Z. Phys. A **307**, 51 (1982).